

# Personal Identification using Minor Knuckle Patterns from Palm Dorsal Surface

Ajay Kumar, Zhihuan Xu

**Abstract**—Finger or palm dorsal surface is inherently revealed while presenting (slap) fingerprints during border crossings or during day-to-day activities like driving, holding arms, signing documents or playing sports. Finger knuckle patterns are believed to be correlated with the anatomy of fingers that involve complex interaction of finger bones, tissues, and skin which can be uniquely identify the individuals. This paper investigates the possibility of using lowest finger knuckle patterns formed on joints between the metacarpal and proximal phalanx bones for the automated personal identification. We automatically segment such region of interest from the palm dorsal images and normalize/enhance them to accommodate illumination, scale and pose variations resulting from the contactless imaging. The normalized knuckle images are investigated for the matching performance using several spatial and spectral domain approaches. We use database of 501 different subjects acquired from the contactless hand imaging to ascertain the performance. This paper also evaluate the possibility of using palm dorsal surface regions, along with their combination with minor knuckle patterns, and provides palm dorsal image database from 712 different subjects for the performance evaluation. The experimental results presented in this paper are very encouraging and demonstrates the potential of such unexplored minor finger knuckle patterns for the biometrics applications.

## 1. INTRODUCTION

Majority of physiological patterns employed for the biometrics identification are closely related to the anatomy of individuals which is relatively unique and believed to be correlated with DNA patterns. The choice of these biometric patterns largely depends on the nature of biometric applications, achievable accuracy, convenience, or restricted to the rarity of patterns available for the forensic analysis [1]. The fingerprint, finger-vein and finger knuckle patterns can be simultaneously acquired and employed for more reliable biometrics identification. In this context, the constrained imaging requirement associated with the acquisition of finger-vein images can add to the total cost and user inconvenience while integrating them with fingerprint based systems. However, the simultaneous acquisition of fingerprint and finger knuckle images can be achieved without any additional inconvenience to users, also at lower cost, with simple addition of an external imaging camera to the existing (slap) fingerprint devices which can simultaneously acquire finger dorsal images and synchronizes the acquisition with external software. Therefore it is important to investigate the uniqueness and stability in the pieces of information which can be recovered from the finger dorsal images. In addition, there are varieties of recorded forensic images (figure 1a-1c) in which only the finger dorsal patterns are available to establish the identity of a suspect. Automated or forensic identification of knuckle patterns has invited very little attention in the literature and several questions relating to uniqueness and/or stability of such patterns are yet to be answered. The work described in this is paper investigates on such problem and examines the possibility of using such second minor

finger knuckle patterns (figure 2) for the human identification.

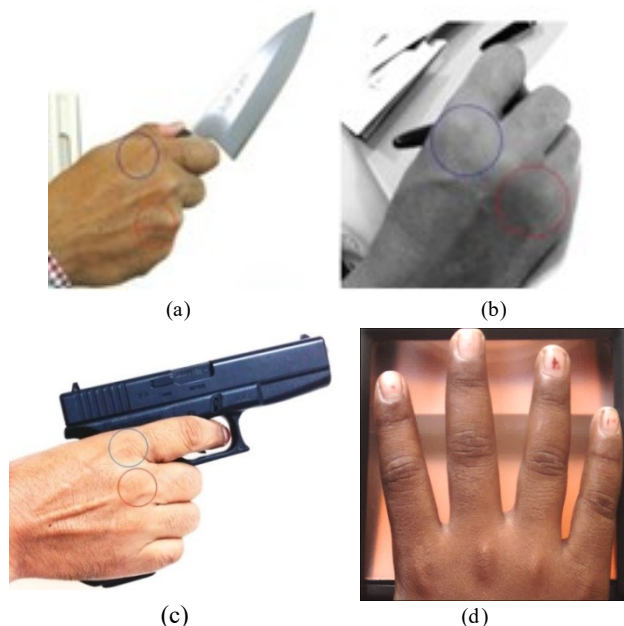


**Figure 1:** (a)-(c) Sample images in which the finger dorsal patterns can be used to ascertain identity of a suspect; (d) Image sample from simultaneous hand dorsal imaging while acquiring fingerprint from slap fingerprint device. The blue and red circles are added to point out the region of interest considered for the investigation in this work.

### 1.1 Motivation and Our Work

The key objective of our work is to investigate the possibility of using finger knuckle patterns, formed between proximal and the metacarpal phalanx bones (metacarpophalangeal joints) of the fingers, for automated human identification. It may be noted that prior work available in the literature has investigated the finger knuckle patterns

Authors are with the Department of Computing, The Hong Kong Polytechnic University, Hung Hom, Kowloon, Hong Kong. Email csajaykr@comp.polyu.edu.hk; zhihuan.xu@polyu.edu.hk.

Manuscript received (insert date of submission if desired). Please note that all acknowledgments should be placed at the end of the paper, before the bibliography.

formed on finger dorsal surface joining middle phalanx and proximal phalanx bones (PIP joints), e.g. [2], [6]-[10], etc. There has also been some work on investigating knuckle patterns formed between distal and middle phalanx bones (DIP joints) reported in the literature [16]. However in the best of our knowledge there has not been any study to ascertain the possibility of exploiting knuckle patterns formed between metacarpal and the proximal phalanx bones (MP joints in figure 2) of fingers for the automated biometric identification. In this paper, we refer such knuckle patterns as the *second* minor finger knuckle patterns to distinguish with the *first* minor knuckle patterns formed on DIP joints and investigated in [16].

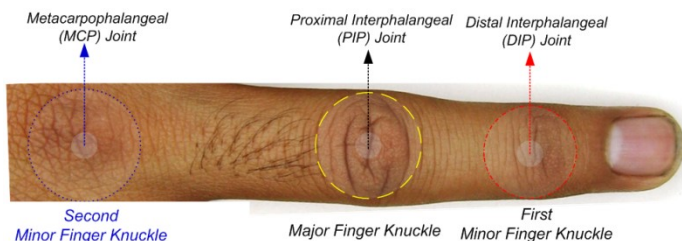


**Figure 2:** Sample finger dorsal image to illustrate prior work in finger knuckle identification and second minor finger knuckle patterns investigated in this work.

The motivation for the investigation detailed in this paper has been two folds: firstly the *second* minor knuckle patterns can be the only<sup>1</sup> piece(s) of evidence available to ascertain the identity of suspect in several images available for the forensic analysis. Therefore investigation into the uniqueness (also stability) of such minor finger knuckle patterns is vital for their usage in forensic identification of suspects. Secondly, such knuckle patterns can be simultaneously acquired using traditional finger knuckle imaging (or even during fingerprint imaging employed at border crossing, e.g. US-VISIT program [23] which uses slap fingerprint imaging devices, by providing additional camera for imaging finger dorsal surface) and used to further improve the performance from conventional finger knuckle (or even fingerprint) identification. The key contributions from this paper can be summarized as follows.

- (a) This paper investigates the finger dorsal skin patterns formed between the metacarpal and the proximal phalanx bones of fingers for their possible use as biometrics trait. The uniqueness of such patterns is ascertained from the experimental results, on the database of 501 subjects (5010 images acquired using contactless imaging), which are highly promising.
- (b) This work also examines simultaneously use of acquired/ available major, first minor and second minor knuckle patterns to achieve superior performance which may not be possible with the use

of any of these knuckle patterns alone. We also investigate possible use of automatically segmented of palm dorsal regions under visible illumination for the biometric applications. This paper also presents preliminary study on the *stability* of such *second* minor finger knuckle patterns using a set of images acquired after an interval of over 2 years.

- (c) This paper also provides a unique database of hand or palm dorsal images acquired from 712 different subjects. This database is also includes dorsal images acquired after a long interval (2-7 years) that will provide valuable insights on the stability of knuckle patterns and its usage on forensic and biometrics applications.

The rest of this paper is organized as follows. Section 2 presents the details on completely automated approach for extracting region of interest (ROI) images. This is followed by brief discussion on the matchers employed for the *second* minor finger knuckle matching. Section 4 provides details on different sets of experimental results while the key conclusions from this paper are summarized in section 5.

## 2. FINGER KNUCKLE IMAGING AND REGION OF INTEREST SEGMENTATION

The key region of interest in this investigation represents

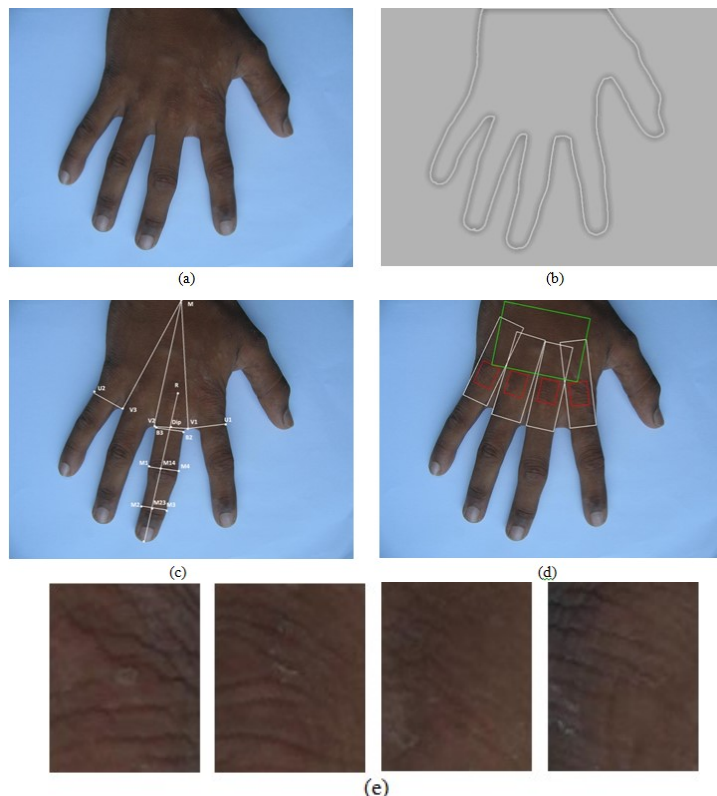
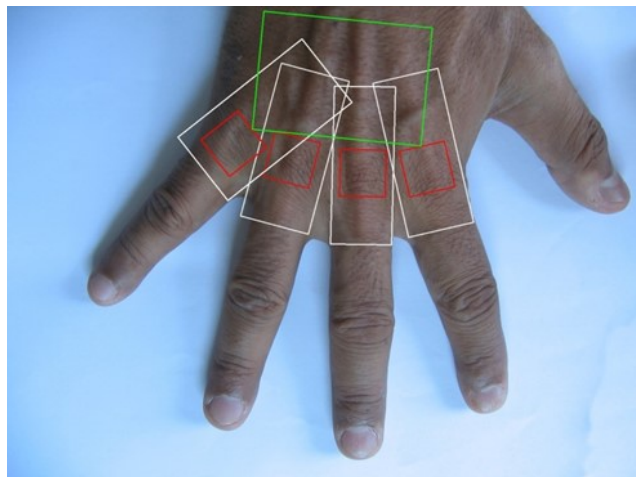


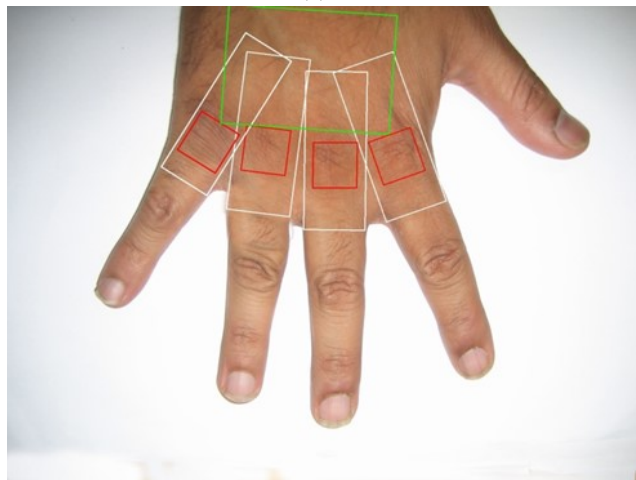
**Figure 3:** Automated segmentation of region of interest (*second* minor finger knuckle); (a) acquired image sample under outdoor illumination, (b) recovered hand contour image (enhanced for easy visualization), and (c) localization of key points. The red squares in figure (d) illustrate the localized *second* minor finger knuckle region and the corresponding segmented knuckle images are shown in (e).

<sup>1</sup> There are known examples [21] of criminal investigations in which the knuckle patterns have been successfully used as a piece of forensic evidence for the prosecution of suspects.

region of image between metacarpal and the proximal phalanx from the finger dorsal surface. This region of interest is automatically segmented from the hand dorsal images employed for this work. The hand dorsal surface images from the right hands of volunteers were acquired using contactless hand imaging. The imaging setup is similar to as the one employed in reference [2]. However in addition to the indoor illumination, the majority of images in the developed database were acquired under outdoor (ambient) illumination.



(a)



(b)

**Figure 4:** Image samples from two volunteers acquired under outdoor (a) and in indoor (b) environment. The red boxes illustrate automatically localized and segmented  $100 \times 100$  pixels ROI to ascertain their possible usage as a biometric trait.

Acquired images are firstly subjected to histogram equalization, binarization (Otsu's method followed by removal of isolated noisy pixels) and used to generate hand contour images as shown in figure 3. The key objective in this work is to evaluate the uniqueness and stability of *second* minor finger knuckle patterns which are formed on the skin surface above the middle phalanx and proximal bone joints of finger dorsal surface. Therefore the automated localization of key points from the hand contour images, similar to as detailed in reference [2], is performed and

utilized in this work (not described here as more details can be referred from [2]). Majority of images employed in this work were acquired under outdoor environment using hand held camera. The distance between the hand held digital camera and hand dorsal surface in contactless imaging is not fixed. Such variations in the distances often generate hand dorsal images with varying scale and therefore scale normalization of the acquired images is performed. This is achieved by normalizing the acquired images to a fixed scale. The scale factor for such normalization is computed from the ratio of distance between the two finger valleys (v1 and v3 in figure 3) and a fixed distance computed from the average of such finger valley distances from sample images (fixed to 325 in all our experiments). The key points corresponding to (four) finger tips and mid-point of two base points for each of the finger are used to further localize the *second* minor finger knuckle region of interest. The line joining finger-tip (top point) and the base point (mid-point of v1 and v2) is further extended by an amount one third of finger length (or by the distance between M23 and M14 in figure 3). This extended point (R in figure 3) is used as the center point of a  $100 \times 100$  pixel square region which is automatically segmented as the *second* minor finger knuckle image. Figure 4 illustrate another two image samples from our database and their automatically localized *second* minor knuckle regions are also highlighted as the red color boxes.

## 2.1 Image Normalization

The finger dorsal images are acquired from the curved 3D knuckle surface and such curves can result in uneven illumination reflections and shadows. Therefore the segmented minor finger knuckle images often have low contrast and illumination variations. The image enhancement steps are essentially required to normalize such illumination variations in the ROI images. The illumination normalization approach used in this work is same as also used in [7]. This approach firstly estimates the average background illumination in the  $16 \times 16$  pixels sub-blocks of the segmented knuckle images. The estimated illumination is then subtracted from the original knuckle image to suppress the influence of uneven illuminations. The resulting image is then subjected to the histogram equalization operation which generates enhanced finger knuckle image for the next or feature extraction stage. Figures 4 (b1)-(b5) and 4(c1)-(c5) illustrate *second* minor finger image samples before and after the image enhancement operations respectively. These images illustrate that employed enhancement approach has been quite effective for enhancing the knuckle creases and curves from the automatically segmented second minor knuckle images.

## 3. FEATURE EXTRACTION AND MATCHING

The *second* minor finger knuckle images after the image enhancement illustrate randomly textured patterns which appears to be quite unique in images from different fingers/ subjects. Such patterns typically consist of creases, lines, and wrinkles of varying thickness, which also varies with the forward movement of respective fingers. A new

approach to match such *second* minor knuckle images is investigated and detailed in the next section. We also comparatively evaluated several matching strategies which have been shown [6], [16]-[19] to be effective in matching palm or major finger knuckle patterns in the literature. These are also briefly described in following.

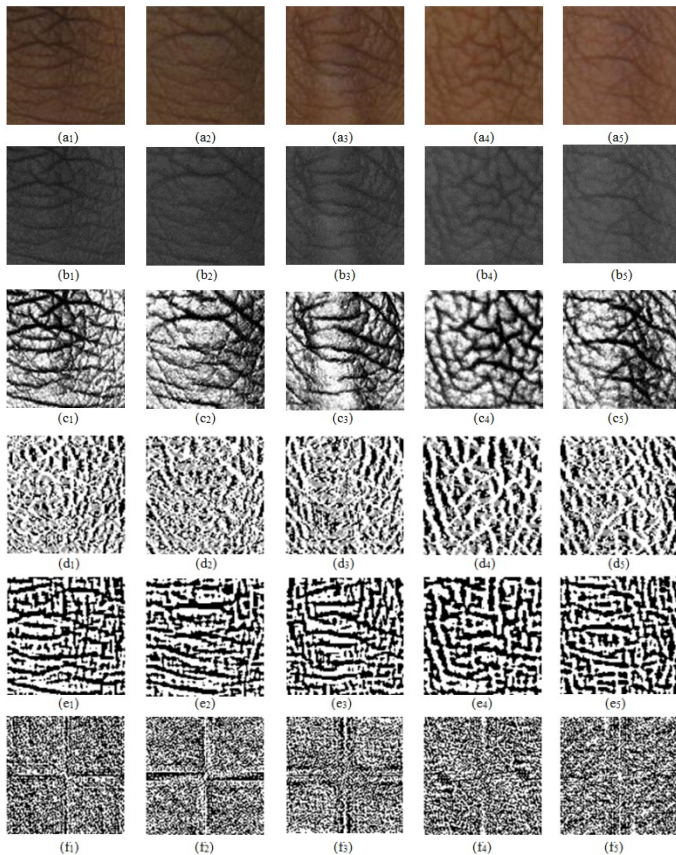


**Figure 5:** Automatically segmented lower or *second* minor knuckle images corresponding to middle finger images of five different subjects in (a<sub>1</sub>-a<sub>5</sub>) respectively. Corresponding grey-level images in (b<sub>1</sub>-b<sub>5</sub>), enhanced images (c<sub>1</sub>-c<sub>5</sub>), *Knuckle-Code* or RLOC representation (d<sub>1</sub>-d<sub>5</sub>), Ordinal representation for 30 deg (e<sub>1</sub>-e<sub>5</sub>), and spectral representation using BLPOC in (f<sub>1</sub>-f<sub>5</sub>).

### 3.1 Local Feature Descriptor

The *second* minor finger knuckle images typically illustrate texture-like details which are random but appears to be quite unique for each of the fingers. These texture patterns can be more effectively and efficiently matched from their spatial feature similarity in local regions. Therefore a new spatial-domain approach [27] to match the knuckle patterns was investigated in this work. A spatial filter is employed to perform convolution with the knuckle images and the quantization of resulting filter response generates respective features corresponding to chosen quantization levels. The two-level quantization can provide compact or smallest size template representation and also generate fast similarity scores using computationally simpler Hamming distances. The features generated from such spatial filtering are expected to encode features which are localized and represents the neighborhood pix-

el information. The size of this spatial filter defines the scope of this neighborhood. The larger (smaller) filter size is expected to encode more global (local) information and vice versa.

Let the shape of this spatial filter be a square to ensure symmetry, then the simplified filter  $f(i, j)$  can be constructed as follows:

$$f(i, j) = \begin{cases} -(2N + 1)^2 + 1 & \text{if } i = 0 \ \&\& \ j = 0 \\ 1 & \text{otherwise} \end{cases} \quad (1)$$

where  $i, j$  is index in the filter,  $i, j \in [-N, N]$ , and  $N$  defines the scope of neighborhood. The filtered response from a point on knuckle surface is essentially the sum of difference between the point and each of its neighboring points. If the local grey level continuity is to be ensured, like in knuckle or natural images, the difference between grey levels from two points which are close to each other should almost be zero. Therefore the sum of them should also be very small and the binary feature  $K(x, y)$  for the point  $(x, y)$  in knuckle image  $I$  can be computed as follows:

$$K(x, y) = \begin{cases} 1 & \text{if } I(x, y) * f(i, j) > 0 \\ 0 & \text{otherwise} \end{cases} \quad (2)$$

where  $*$  represents pixel-wise convolution operation. When the encoded feature from (2) is one, the local knuckle shape is expected to concave else the described shape is more likely to be convex.

It is generally believed that the gradient of descriptors can offer more powerful capability to describe the feature. Therefore the gradient version of filter  $f(i, j)$  in (1) is expected to generate more powerful feature descriptor. We partition the neighbors of a given point  $(x, y)$  into two subsets whose spatial extent or size is the same. For all the points or image pixels in the two subsets, we subtract their value from  $I(x, y)$ . After computing the sum of points' values for each subset, the gradient is defined as the difference between these two respective/ sum results. Let these two subsets be represented as  $D_1$  and  $D_2$ , then the gradient filter  $g(i, j)$  obtained from  $f(i, j)$  can be defined as follows:

$$g(i, j) = \begin{cases} -1 & \text{if } point(i, j) \in D_1 \\ 1 & \text{otherwise} \end{cases} \quad (3)$$

There can be several possibilities to explore the spatial extent of partitions  $D_1$  and  $D_2$ . In this work we only considered simplified partitions to define  $g(i, j)$  as follows:

$$g(i, j) = \begin{cases} 1 & \text{if } abs(i) < abs(j) \\ -1 & \text{if } abs(i) > abs(j) \\ 0 & \text{if } abs(i) = abs(j) \end{cases} \quad (4)$$

where  $i, j$  is index in the filter with  $i, j \in [-N, N]$  and  $abs(\cdot)$  is the absolute operation. The matching distance  $S_f$  between the two feature matrix, *i.e.*, one obtained from the gallery ( $G$ ) and the probe ( $E$ ), is computed as follows:

$$S_f = \frac{1}{(n-q)(m-p)} \sum_{y=1}^{m-p} \sum_{x=1}^{n-q} XOR(G(x, y), E(x, y)) \quad (5)$$

where  $XOR(G, E)$  is the Boolean XOR operator that computes Hamming distance between two binarized template  $G$  and  $E$  while  $m$  and  $n$  denotes the spatial size of these templates. In order to accommodate possible translations between the knuckle surface, we translate the binarized

templates of the probe in horizontal  $q$  and vertical direction  $p$  and perform multiple matches. These translations are performed in two steps for four directions (left, right, up, down) in steps of two pixels. The best or smallest of Hamming distance among these translations is used as final similarity score  $s_f$  (5) between the two matched templates.

### 3.2 Band Limited Phase Only Correlation

Another possible approach to match these knuckle patterns is to compute their similarity or correlation from their spectral representations. Such an approach has shown to offer more accurate results [16]-[17] and was therefore attempted to match *second* minor knuckle images. This approach *only* uses phase information recovered from the 2D discrete Fourier transform (DFT) of the segmented knuckle images and therefore least sensitive to the translation/ rotational changes. In order to minimize the influence noise, only a band of frequency in the DFT representation is employed for the matching. This approach detailed in [17] is briefly summarized in the following.

Let 2D DFT of two  $P \times Q$  pixels normalized knuckle images, say  $S_1(x, y)$  and  $S_2(x, y)$ , be respectively represented as  $F_1(k_1, k_2)$  and  $F_2(k_1, k_2)$ . These 2D DFTs can be computed as follows:

$$F_1(k_1, k_2) = \sum_{x,y} S_1(x, y) e^{-\frac{i2\pi x k_1}{P}} e^{-\frac{i2\pi y k_2}{Q}} = B_{F_1} e^{-i\phi_{F_1}(k_1, k_2)} \quad (6)$$

$$F_2(k_1, k_2) = \sum_{x,y} S_2(x, y) e^{-\frac{i2\pi x k_1}{P}} e^{-\frac{i2\pi y k_2}{Q}} = B_{F_2} e^{-i\phi_{F_2}(k_1, k_2)} \quad (7)$$

where  $B_{F_1}$  and  $B_{F_2}$  are the amplitudes,  $\phi_{F_1}(k_1, k_2)$  and  $\phi_{F_2}(k_1, k_2)$  are the phase component of normalized knuckle image  $S_1(x, y)$  and  $S_2(x, y)$  respectively. The cross-correlation  $C_{F_1 F_2}(k_1, k_2)$  between two phase components from (6) and (7) is computed as follows:

$$C_{F_1 F_2}(k_1, k_2) = \frac{F_1(k_1, k_2) \overline{F_2(k_1, k_2)}}{|F_1(k_1, k_2) F_2(k_1, k_2)|} = e^{-i\{\phi_{F_1}(k_1, k_2) - \phi_{F_2}(k_1, k_2)\}} \quad (8)$$

where  $\overline{F_2(k_1, k_2)}$  is the complex conjugate of  $F_2(k_1, k_2)$  and  $\{\phi_{F_1}(k_1, k_2) - \phi_{F_2}(k_1, k_2)\}$  represents difference in phase components between two matched knuckle images. The phase only correlation between two knuckle images is estimated from the inverse 2D DFT of  $C_{F_1 F_2}(k_1, k_2)$  as follows:

$$c_{l_1 l_2}(x, y) = \frac{1}{PQ} \sum_{k_1, k_2} C_{F_1 F_2}(k_1, k_2) e^{i2\pi x k_1 / P} e^{i2\pi y k_2 / Q} \quad (9)$$

The band limited correlation between phase representations from two images is obtained by limiting  $k_1$  and  $k_2$  in (9) to some limit instead to  $P$  and  $Q$  respectively.

### 3.3 Local Radon Transform

Matching knuckle images using Local Radon Transform (LRT), referred to as RLOC [19] or *KnuckleCode* representation in [6], has shown to be quite effective in accurately matching the major knuckle patterns and was therefore also evaluated in this work. This approach effectively encodes the local orientation of curved lines and knuckle creases into one of the dominant orientations which is represented using a three bit binary code and such binarized templates are matched using the Hamming dis-

tance. The details of this approach can be found in reference [6], [13] or [19]. The key advantage of this approach is that it produces smaller template size [13] and is computationally efficient in generating templates than BLPOC, and also the ordinal representation approach considered for the performance comparison. Another approach referred as (fast) CompCode [13], which is quite similar in encoding local knuckle crease orientations but using even Gabor filters, was also evaluated for the comparative performance.

### 3.4 Ordinal Representation

The ordinal measures typically compute measurements that are based on the relative distances [20]. The ordinal representation of textured like surface such as palm and iris has shown to offer promising results and therefore this method was also evaluated to ascertain its accuracy in matching the knuckle images. Similar to as detailed in reference [18], two orthogonal Gaussian filters oriented at 0, 30 and 60 degrees are utilized to generate binarized feature templates. The Hamming distance between resulting feature templates is employed to generate match scores between the knuckle images matches.

## 4. EXPERIMENTS AND RESULTS

The experiments were performed in several phases to ascertain the usefulness of *second* minor finger knuckle patterns for the biometric authentication. We acquired hand dorsal images from 501 different subjects using contactless hand imaging. The images were acquired from the right hand of the volunteers under indoor or outdoor environment. All the acquired images were used to automatically segment  $100 \times 100$  pixel ROI corresponding to *second* minor finger knuckle region as described in section 2. These images were enhanced and subjected to the feature extraction using three matchers as discussed in section 3. The band limiting threshold for BLPOC was fixed to 0.6 for all the experiments. The line width and length of one and seven pixel was respectively fixed for all experiments in RLOC (the filter size was  $11 \times 11$ ). Two Gaussian filters ( $\delta_x = 3$ ,  $\delta_y = 1$ ) of size  $11 \times 11$  pixels were utilized to compute ordinal representations of the segmented knuckle for the matching. Figure 5 illustrates some sample knuckle images and corresponding template images for respective enhanced knuckle images. The templates corresponding to the computationally simpler method detailed in section 3.1 are shown in figure 6.

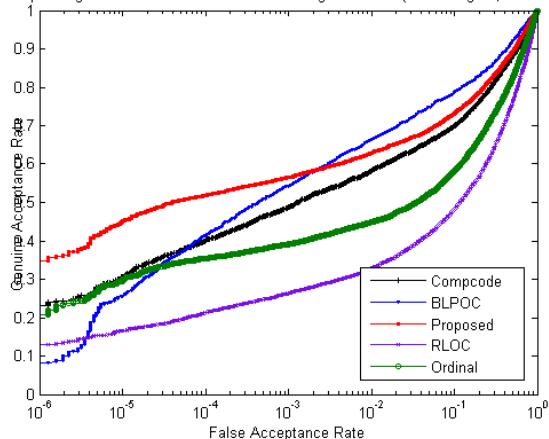


**Figure 6:** Typical samples of templates generated from six different subjects' second minor knuckle using local features detailed in section 3.1.

The first sets of experiments were performed to ascertain the suitability of matcher and its performance for the *second*

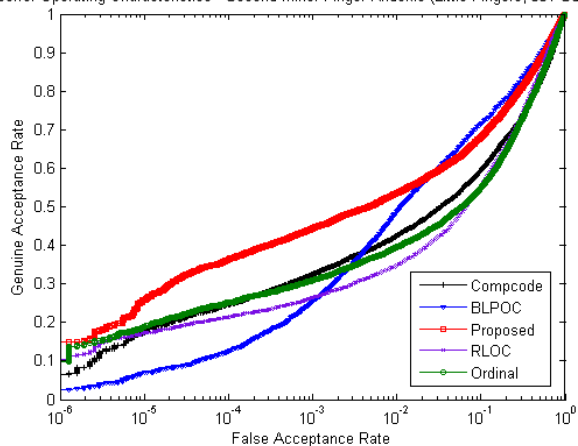
minor finger knuckle patterns. We utilized five images from each of the four fingers, for every subject, and employed relatively challenging protocol (all-to-all instead of leave-one-out) for matching *second* minor knuckle images. Therefore 5010 ( $501 \times 10$ ) genuine scores and 1252500 ( $501 \times 5 \times 500$ ) impostor scores were computed. The matching performance was evaluated using the receiver operating characteristic (ROC). The ROC corresponding to the *index*, *little*, *middle*, and *ring* finger is shown in figure 7(a), (b), (c) and (d) respectively. It can be ascertained from these ROCs that the local feature based matcher evaluated in this work performs the best among five matchers considered for the

Receiver Operating Characteristics - Second Minor Finger Knuckle (Index Fingers, 501 Subjects)



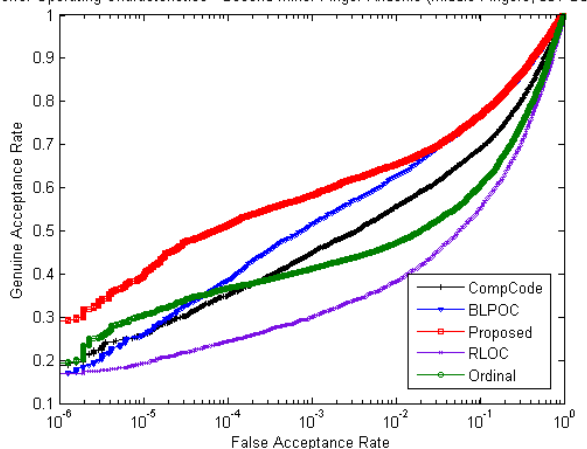
(a)

Receiver Operating Characteristics - Second Minor Finger Knuckle (Little Fingers, 501 Subjects)



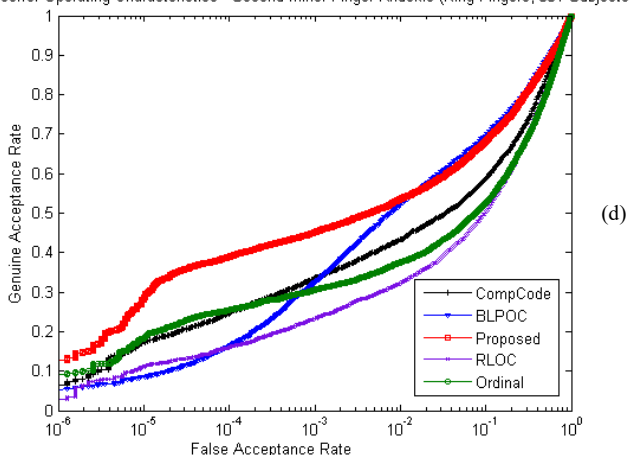
(b)

Receiver Operating Characteristics - Second Minor Finger Knuckle (Middle Fingers, 501 Subjects)



(c)

Receiver Operating Characteristics - Second Minor Finger Knuckle (Ring Fingers, 501 Subjects)



(d)

**Figure 7:** The ROC for matching *second* minor finger knuckle images from 501 different subjects (a) index fingers, (b) little, (c) middle and (d) ring fingers using five different matchers considered in this work

performance comparison. The equal error rate (EER) from different matchers is also presented in table 1. In terms of EER, the performance of this approach can be considered to be similar to the BLPOC although BLPOC marginally performs better in some cases. It should however be noted that ROC rather than EER is widely considered as the reliable criterion for performance comparison. The complexity of BLPOC that requires computation of 2DFFT is also significantly high. Therefore we employed only the outperforming matcher (figure 7) using local features for other further experiments reported in this paper.



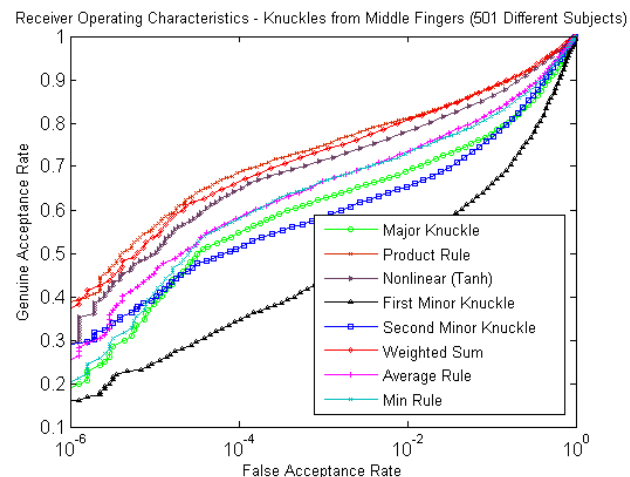
**Figure 8:** A typical palm dorsal image from the database used to automatically segment *first* minor (yellow boxes) and major (red boxes) from all four fingers.

The second sets of experiments were performed to ascertain possible performance improvement using the combination of simultaneously available/acquired *first*, *second* minor and major knuckle patterns from the finger dorsal images. In addition to *second* minor patterns, all the finger images acquired from 501 subjects also illustrate major and first minor [24] finger knuckle patterns. These regions were also automatically segmented using the approach detailed in section 2 [2]. Figure 8 shows a typical palm dorsal image from our

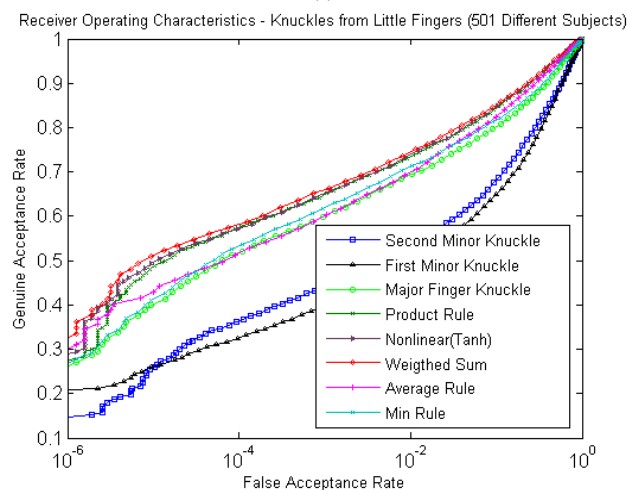
**Table 1:** Comparative EER (%) from *second* minor knuckle matching.

	<i>Index</i>	<i>Middle</i>	<i>Ring</i>	<i>Little</i>
Ours	0.20875	0.18474	0.23173	0.22838
BLPOC	0.1792	0.1858	0.2208	0.2146
RLOC	0.33478	0.30035	0.30954	0.28247
Ordinal	0.28208	0.27499	0.30716	0.28601
Compcode	0.22113	0.23106	0.28382	0.28146

database and the segmented knuckle regions for each of the fingers. The ROC for the individual and score-level combination of knuckle patterns from 501 subjects ring, index, middle and little fingers are shown in figure 9(a), (b), (c) and (d) respectively. These results indicate that combination of knuckle patterns can achieve improved performance which cannot be achieved by *first* minor, *second* minor or major knuckle patterns alone. We attempted several simplified score-level combination approaches [27] to combine major and minor knuckle patterns. It can be observed that the score level combination using weighted sum can generate superior results in most cases.



(c)

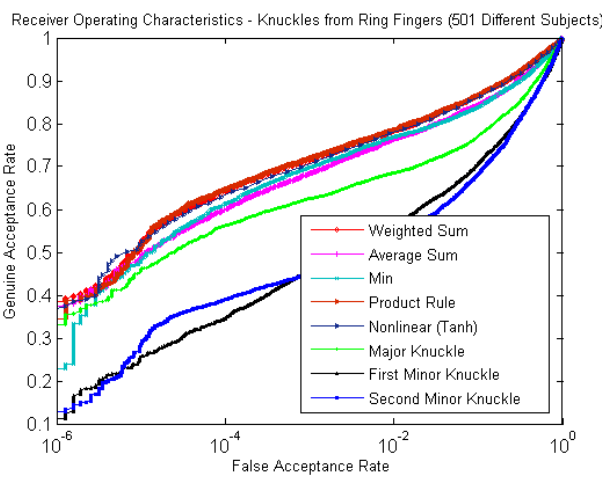


(d)

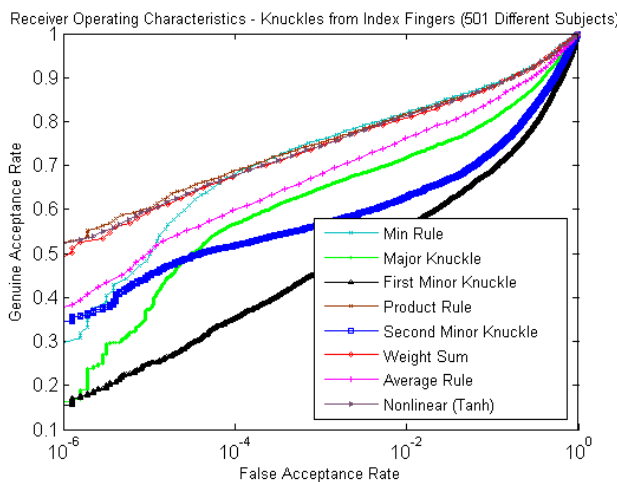
**Figure 9:** The ROC for the combination of minor and major finger knuckle images from 501 different subjects (a) index fingers, (b) little, (c) middle and (d) ring fingers.

In addition to hand dorsal images from 501 different subjects, we also acquired four finger dorsal images from another 211 subjects. These additional images only show first minor and major knuckle regions and do not illustrate *second* minor finger knuckle regions. Therefore these images were not utilized for the earlier set of experiments. The combined database of 712 subjects finger dorsal images was also used to investigate the matching performance, using automatically segmented first minor and major knuckle images, to benchmark the performance for further work. The ROCs from these set of experiments using five images from 712 subjects (7120 genuine and 12525000 impostor scores) is shown in figure 10. This database from 712 different subject's right hands is the largest database employed so far the matching (figure 10) finger knuckle patterns and is publicly [26] or freely made available for further work.

Another set of experiments were performed to ascertain if the palm (or palmprint) dorsal region (green color rectangle region shown in figure 3 and 4) available under visible illumination can also be used for the biometric matching. Each of the hand dorsal images includes palm dorsal region, acquired under visible illumination, and this region typically illustrate textured-like surface



(a)



(b)

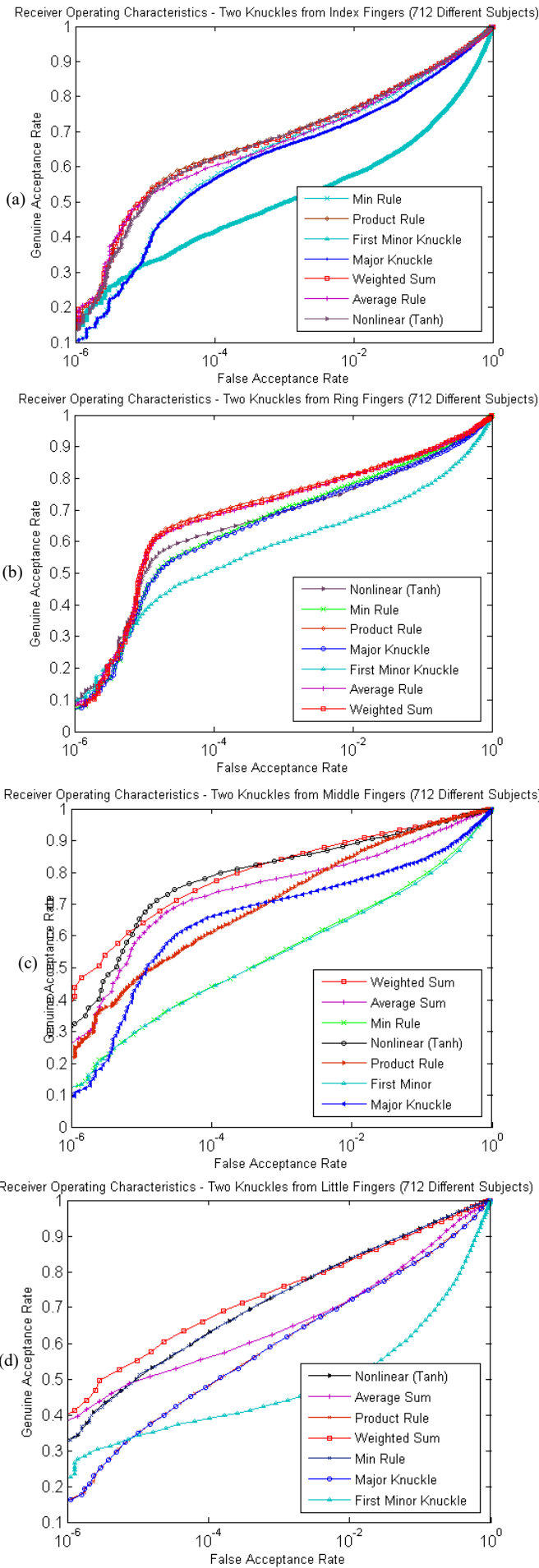
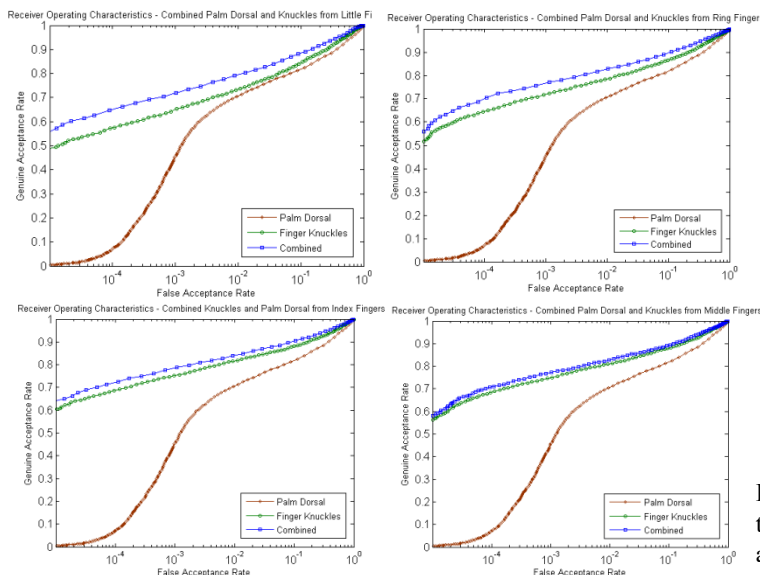


**Figure 10:** The ROC for the combination of first minor and major finger knuckle images from 712 different subjects (a) index, (b) little, (c) middle and (d) ring fingers.



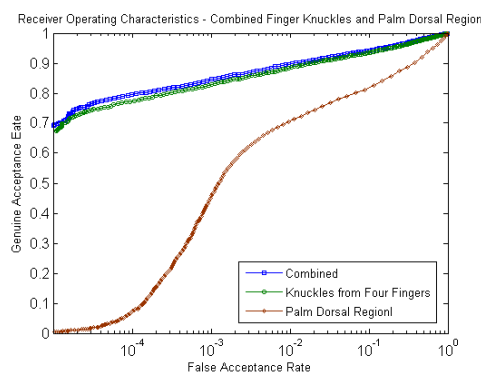
**Figure 11:** Typical palm dorsal image samples from nine different subjects in the database.

with distinctive vascular patterns, skin pigmentation and texture which appears to be quite different among different subjects. Therefore it is judicious to examine possible use of this region for the biometric matching. We automatically segment this palm dorsal region, using the key points generated during the knuckle segmentation, and employ this region for matching like we did for the knuckle images in previous experiments. In figure 11 several automatically segmented palm dorsal image samples from our database are reproduced and such palm dorsal images were investigated for improving matching performance from simultaneously segmented knuckle images. The ROC from 501 different subjects (automatically segmented) palm dorsal matching, using same protocol and method as for figure 7-8, is shown in figure 12. The EER for matching palm dorsal regions was 0.15607 (0.1685 using BLPOC). It can be observed that the matching of palm dorsal region images, can also achieve promising performance particularly on larger database from 501 different subjects. This figure also illustrates the improvement in performance using the match score level combination of respective finger knuckles with palm dorsal images. This combination resulted in EER of 0.096, 0.1054, 0.0994, 0.1080 for *index*, *middle*, *ring* and *little* finger respectively. The performance improvement is observed to be consistent, although not very significant. The palm dorsal region images also have high potential for forensic identification of suspects or in biometric applications involving access by smaller number of subjects. Our results should be considered preliminary indicating its promises and the need for further work.



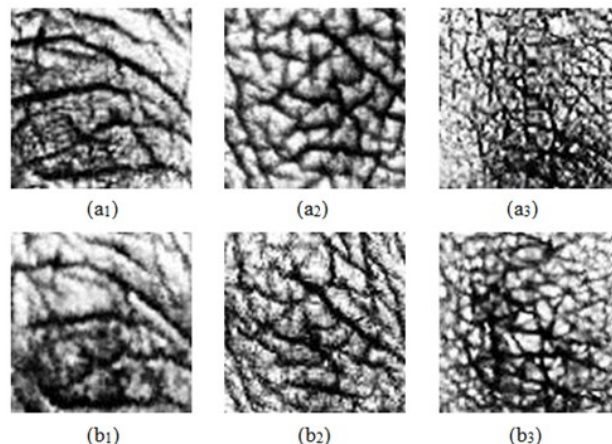
**Figure 12:** The ROC from the palm dorsal regions and its combination with three knuckles for (a) little, (b) ring, (c) index and (d) middle finger respectively.

There can be several methods to combine palm dorsal region match scores with three different knuckles from the four fingers of same hand/ subject that have been used in previous (figure 9) experiments. Figure 13 illustrates the matching performance using a weighted combination of combined knuckle matching scores from four fingers with the palm dorsal region matching scores. The marginal improvement in performance with the addition of palm dorsal region can be observed from this figure. The EER corresponding to this combination is 0.628. More advanced fusion schemes that can adaptively combine multiple finger knuckle match scores and palm dorsal region match scores are expected to deliver more accurate performance and should be explored in further work.



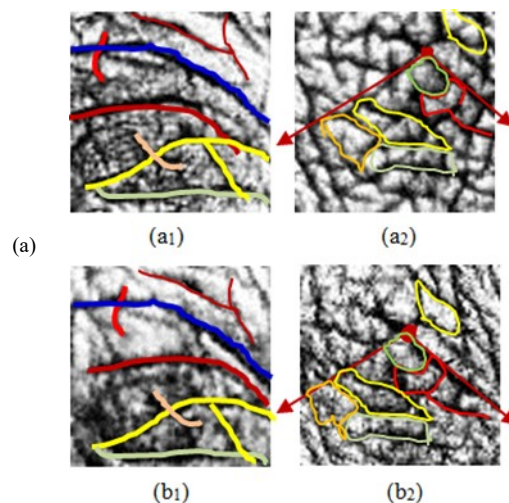
**Figure 13:** The ROC using combination of knuckle and palm dorsal matching from all four fingers of 501 different subjects.

We also evaluated the stability of second *minor* knuckle patterns from images acquired over relatively large interval for its possible usage in the forensic identification of suspects. In order to ascertain such stability of *second* minor finger knuckle patterns, we employed two-session hand dorsal images acquired during the four years from 43 different subjects. Majority of subjects in this database



**Figure 14:** Enhanced image samples corresponding to three different subject's *second* minor finger knuckle images acquired over an interval of 2 years. These image samples not only illustrate stability of knuckle creases or patterns *but* also include the variations introduced due to contactless imaging under ambient illumination.

had second session acquired after an interval of at least two years. Some of these image samples are shown in figure 14-15. Some subjects in this dataset were students in teenage who had noticeable physiological growth while some were in mid-thirties (figure 14 - a<sub>1</sub>) whose knuckle lines and creases were relatively stable and even could be matched manually. We also evaluated the automated matching accuracy from matching two (but long) session *second* minor knuckle images. The number of genuine score in this set of experiments was 215 (43×5) while the number of impostor scores was 11180 (43×5×42). The ROC corresponding to four different fingers are shown in figure 15. It should be noted that the error or degradation in performance is not *just* due to alterations in *second* minor knuckle patterns but also due to localization and segmentation errors in the lower quality images acquired under contactless imaging. These two-session images are also made publicly available and figure 14-15 underline the need for further work to develop matching techniques that can accommodate knuckle curve and crease deformations in such images.



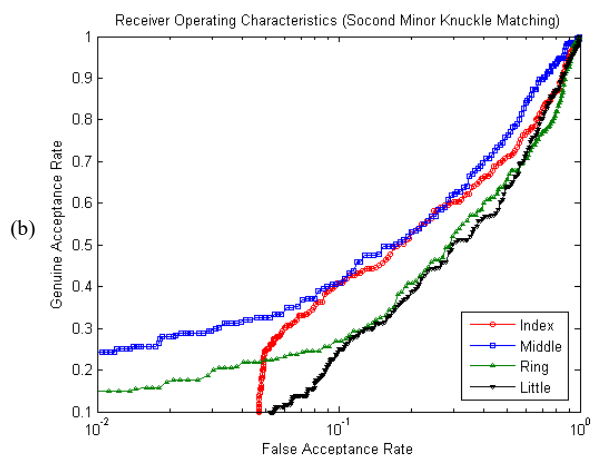


**Figure 15:** (a) Manual matching of *second* minor finger knuckle patterns for the first two subjects in figure 14. The knuckle curves and creases are easy to be matched for subject  $a_1$ , but more difficult for subject  $a_2$  and  $a_3$  (match is not shown). (b) The ROC from matching two-session *second* minor finger knuckle images using completely automated approach

## 5. CONCLUSIONS AND FURTHER WORK

This paper has investigated the possibility of using *second* minor finger knuckle image for the personal identification. The approach described in this paper is completely automated and uses contactless imaging which is expected to produce/ accommodate large variations in images. The experimental results on the image database from over 500 subjects presented in this paper suggest great potential for the *second* minor knuckle patterns to be employed as a biometric identifier. We also investigated a computationally simpler method of matching such knuckle patterns using local features and achieved outperforming results. The experimental results presented in this paper also suggest that the combination of simultaneously acquired/ available major, first minor and *second* minor knuckle patterns can achieve superior performance which is not possible from any of the three finger knuckle patterns alone. The work detailed in this paper also investigated the potential for visible illumination palm dorsal images as a biometric identifier. Automatically segmented images from 501 subjects, with significant majority of them acquired under outdoor illumination, were used to ascertain matching capability from such potential identifier and encouraging results were obtained. Our results also demonstrated that the combination of finger knuckle patterns and simultaneously extracted palm dorsal regions can be used to further improve knuckle matching performance. The results presented from these set of experiments should be considered preliminary, indicating great potential for this region to serve as biometric, and require further work to achieve more accurate performance.

A workshop version of this paper appears in reference [22] and presented some of experimental results on a *proprietary* database of 110 subjects and with the same minor knuckle matcher employed in [24]. This paper has how-

ever presented experimental results on much larger database from 501 different subjects, using a superior approach (section 3.1), and also provides entire database from 712 different subjects in the public domain. This database has been acquired from large number of subjects, also includes long interval images as much as over 7 year interval, and will help to advance further research required in this area. The experiments on larger database using various combinations of first, second minor and major knuckle patterns, along with the new investigations on the simultaneously extracted palm dorsal regions as a biometric identifier, are some of other notable contributions in this paper over [22]. The strength of this work lies in completely automated evaluation of *second* minor knuckle patterns which have not yet attracted attention in biometrics. The attempt to match *second* minor knuckle patterns has generated promising results but requires further work to improve accuracy from such matching. The experimental results presented in this paper should be interpreted in the context of largest (so far) database employed, challenging protocol and completely automated approach employed for the knuckle segmentation. The automated segmentation approach for knuckle images employed in this paper does not generate perfect segmentation of region of interest in many cases. This is largely due to large illumination variations under the outdoor environment and further effort to improve the segmentation accuracy is expected to further improve the matching performance and is suggested for further work. The image considered in this work largely uses images when palm dorsal images are acquired from the stretched palms. However higher variations in knuckle patterns is expected when images from non-stretched palm or bending of fingers is acquired and further extension of this work is expected to develop database/ algorithms to match images with such variations. The matching accuracy from two session *second* minor knuckle images is also quite poor and needs further work for its use in the forensic applications.

## 6. REFERENCES

- [1] Y. Tang and N. Srihari, "Likelihood ratio estimation in forensic identification using similarity and rarity," *Pattern Recognition*, vol. 47, no. 3, pp. 945-958, Mar. 2014.
- [2] A. Kumar and Ch. Ravikanth, "Personal authentication using finger knuckle surface", *IEEE Trans. Info. Forensics & Security*, vol. 4, no. 1, pp. 98-110, Mar. 2009
- [3] AADHAR - Communicating to a billion, *Unique Identification Authority of India, An Awareness and Communication Report*, ACSAC, [http://uidai.gov.in/UID\\_PDF/Front\\_Page\\_Articles/Events/AADHAAR\\_PDF.pdf](http://uidai.gov.in/UID_PDF/Front_Page_Articles/Events/AADHAAR_PDF.pdf)
- [4] A. Kumar and Y. Zhou, "Human identification using finger images," *IEEE Trans. Image Processing*, vol. 21, pp. 2228-2244, April 2012.
- [5] S. Ribaric and I. Fratric, "A Biometric identification system based on eigenpalm and eigenfinger Features", *IEEE Trans. Pattern Anal. Mach. Intell.*, vol. 27, no. 11, Nov. 2005.
- [6] A. Kumar and Y. Zhou, "Human identification using knuckle-

- codes,” *Proc. 3rd Intl. Conf. Biometrics, Theory and Applications*, Washington D. C., BTAS'09, pp. 147-152, Sep. 2009.
- [7] K. Sricharan, A. Reddy and A. G. Ramakrishnan, “Knuckle based hand correlation for user verification,” *Proc. SPIE* vol. 6202, *Biometric Technology for Human Identification III*, P. J. Flynn, S. Pankanti (Eds.), 2006. doi: 10.1117/ 12.666438
- [8] M. Choraś and Rafał Kozik, “Contactless palmprint and knuckle biometrics for mobile devices,” *Pattern Analysis & Applications*, vol. 1, no. 15, 2012.
- [9] L.-q. Zhu and S.-y. Zhang, “Multimodal biometric identification system based on finger geometry, knuckle print, and palm print,” *Pattern Recogn. Letters*, vol. 31, pp. 1641-1649, Sep. 2010.
- [10] L. Zhang, L. Zhang, D. Zhang and H. Zhu, “Online finger-knuckle-print verification for personal authentication,” *Pattern Recognition*, vol. 43, no. 7, pp. 2560-2571, Jul. 2010
- [11] T. Ojala, M. Pietikäinen, and T. Mäenpää, “Multiresolution gray-scale and rotation invariant texture classification with local binary patterns,” *IEEE Trans. Pattern Anal. Mach. Intell.*, vol. 24, no. 7, pp. 971-987, 2001.
- [12] H. Jin, Q. Liu, H. Lu, X. Tong, “Face detection using improved LBP under Bayesian framework,” *Proc. ICIG*, pp. 306-309, Dec. 2004.
- [13] Q. Zheng, A. Kumar, G. Pang, “Suspecting less Suspecting less and achieving more: New insights on palmprint identification for faster and more accurate palmprint matching,” *IEEE Trans. Information Forensics & Security*, vol. 11, pp. 633-641, Mar. 2016.
- [14] D. G. Joshi, Y. V. Rao, S. Kar, V. Kumar, and R. Kumar, “Computer vision based approach to personal identification using finger crease patterns,” *Pattern Recognition*, vol. 31, pp. 15-22, Jan. 1998.
- [15] D. L. Woodard and P. J. Flynn, “Finger surface as a biometric identifier”, *Computer Vision and Image Understanding*, vol. 100, no. 3, pp. 357-384, Dec. 2005.
- [16] A. Kumar, “Can we use minor finger knuckle images to identify humans?,” *Proc. BTAS 2012*, pp. 787-87g, Sep. 2012.
- [17] K. Ito, T. Aoki, H. Nakajima, K. Kobayashi, T. Higuchi, “A palmprint recognition algorithm using phase-only correlation,” *IEICE Trans. Fundamentals of Electronics, Communications and Computer Sciences*, vol. E91-A, pp. 1023-1030, April 2008.
- [18] Z. Sun, T. Tan, Y. Wang, S. Z. Li, “Ordinal palmprint representation for personal identification,” *Proc. CVPR 2005*, pp. 279-284, 2005.
- [19] W. Jia, D.-S. Huang, D. Zhang, “Palmprint verification based on robust line orientation code,” *Pattern Recognition*, vol. 41, pp. 1504-1513, May 2008.
- [20] P. Sinha. “Qualitative representations for recognition,” *Biologically Motivated Computer Vision*, pp 249–262. Springer, 2002.
- [21] Bromley Paedophile Dean Hardy Jailed for 10 Years, *Bromley Times*, Jan. 2012.  
[http://www.bromleytimes.co.uk/news/courtcrime/bromley\\_paedophile\\_dean\\_hardy\\_jailed\\_for\\_10\\_years\\_1\\_1176957](http://www.bromleytimes.co.uk/news/courtcrime/bromley_paedophile_dean_hardy_jailed_for_10_years_1_1176957)
- [22] A. Kumar and Z. Xu, “Can we use second minor finger knuckle patterns to identify humans?,” *Proc. CVPR 2014*, CVPR'W14, pp. 106 – 112, Columbus, Ohio, June 2014.
- [23] US-VISIT Program, Department of Homeland Security, USA, [https://www.dhs.gov/xlibrary/assets/usvisit/usvisit\\_edu\\_10\\_fingerprint\\_consumer\\_friendly\\_content\\_1400\\_words.pdf](https://www.dhs.gov/xlibrary/assets/usvisit/usvisit_edu_10_fingerprint_consumer_friendly_content_1400_words.pdf)
- [24] A. Kumar, “Importance of being unique from finger dorsal patterns: exploring minor finger knuckle patterns in verifying human identities,” *IEEE Trans. Info. Forensics & Security*, vol. 8, pp. 1288-1298, Aug. 2014.
- [25] *The Hong Kong Polytechnic University Contactless Hand Dorsal Images Database*, available at <http://www.comp.polyu.edu.hk/~csajaykr/knuckleV2.htm>.
- [26] A. W. K. Kong and D. Zhang, “Competitive coding scheme for palmprint verification”, *Proc. 17th ICPR*, Washington, DC, pp. 1051-4651, 2004.
- [27] A. Kumar and Q. Zheng, “A method and device for contactless biometrics identification,” *Pending U. S. Patent No. 62032528*, Aug. 2014.
- [28] A. Kumar and D. Zhang, “Personal recognition using hand-shape and texture,” *IEEE Trans. Image Process.*, vol. 15, no. 8, pp. 2454-2461, Aug. 2006.